

Bridging Planning and Execution: Multi-Agent Path Finding Under Real-World Deadlines

Jingtian Yan*, Shuai Zhou*, Stephen F. Smith, Jiaoyang Li

Abstract—The Multi-Agent Path Finding (MAPF) problem aims to find collision-free paths for multiple agents while optimizing objectives such as the sum of costs or makespan. MAPF has wide applications in domains like automated warehouses, manufacturing systems, and airport logistics. However, most MAPF formulations assume a simplified robot model for planning, which overlooks execution-time factors such as kinodynamic constraints, communication latency, and controller variability. This gap between planning and execution is problematic for time-sensitive applications. To bridge this gap, we propose REMAP, an execution-informed MAPF planning framework that can be combined with leading search-based MAPF planners with minor changes. Our framework integrates the proposed ExecTimeNet to accurately estimate execution time based on planned paths. We demonstrate our method for solving MAPF with Real-world Deadlines (MAPF-RD) problem, where agents must reach their goals before a predefined wall-clock time. We integrate our framework with two popular MAPF methods, MAPF-LNS and CBS. Experiments show that REMAP achieves up to 20% improvement in solution quality over baseline methods (e.g., constant execution speed estimators) on benchmark maps with up to 300 agents.

I. INTRODUCTION

The Multi-Agent Path Finding (MAPF) problem seeks to find collision-free paths for multiple agents in a shared environment while optimizing objectives such as the sum of costs or makespan. This problem is a fundamental challenge in settings such as automated warehouses [1], traffic intersections [2], and airport logistics [3]. State-of-the-art MAPF methods can efficiently coordinate hundreds of agents, making MAPF a promising solution for these domains. However, many real-world MAPF applications operate under strict temporal constraints. For instance, in e-commerce warehouses, promises of same-day or even one-hour delivery require robots to transport items within tight deadlines [4]. This requires MAPF planners to generate paths that are not only collision-free but also executable within real-world time constraints.

To address the MAPF problem with time constraints, recent work has proposed MAPF with Deadlines (MAPF-DL) [4], [5], where agents must reach goals before specified deadlines. These methods extend standard MAPF methods by incorporating deadline constraints into the planning process, ensuring that planned paths can theoretically complete before deadlines. However, they assume that planning timesteps directly correspond to real-world execution time, while most

MAPF formulations use simplified robot models and overlook execution-time factors such as kinodynamic constraints and controller variability. This planning-execution gap can lead to deadline violations even when following theoretically deadline-compliant paths. Although not specifically designed to address this gap, some methods [6], [7] were proposed to bridge it by integrating more accurate robot models during planning or post-processing. However, these models still require accurate characterization of robot dynamics and may not fully account for execution-time uncertainties such as communication latency and controller variability. A straightforward alternative is to simulate the execution of a MAPF solution and directly measure the resulting execution times. While execution frameworks like the Action Dependency Graph (ADG) [1] can support robust execution of MAPF solutions, this process is computationally expensive and impractical to integrate during planning. To the best of our knowledge, no existing work jointly addresses both deadline-aware planning and the planning-execution gap in MAPF.

To solve this problem, we propose **Real-world Execution-time-informed Multi-Agent Planning (REMAP)**, a framework designed to bridge the planning-execution gap for MAPF applications under real-world time constraints. REMAP can be integrated with leading search-based MAPF planners through minor modifications, enabling them to account for execution time during planning. Specifically, we propose ExecTimeNet, a Transformer-GNN-based neural network, to predict execution time for each agent using the paths found by the MAPF planner. These predictions are then used to guide the MAPF search process. Our main contributions are: (1) We introduce the MAPF under Real-world Deadlines (MAPF-RD) problem, highlighting how the planning-execution gap poses challenges in such problems; (2) We propose REMAP, a framework that enables leading families of search-based MAPF planners to handle the MAPF-RD problem; (3) We design ExecTimeNet, a neural model that accurately predicts execution times and generalizes to unseen maps; (4) Our experiments in a physics-engine-based simulator show that REMAP can achieve up to a 20% improvement in solution quality over baseline methods (e.g., constant execution speed estimators) on benchmark maps with up to 300 agents..

II. BACKGROUND

We first define the Multi-Agent Path Finding under Real-world Deadlines problem and then review related works.

A. Problem Formulation

Definition 1 (Multi-Agent Path Finding): We define the MAPF problem on an undirected graph $\mathcal{G} = (V, E)$, where V

This paper was produced by the IEEE Publication Technology Group. They are in Piscataway, NJ.

Manuscript received April 19, 2021; revised August 16, 2021.

J. Yan, S. Zhou, S. Smith, and J. Li are with Robotics Institute, Carnegie Mellon University, Pittsburgh, PA 15213, USA (email: jingtian, shuaizhou, ssmith@andrew.cmu.edu, jiaoyangli@cmu.edu).

Digital Object Identifier (DOI): see top of this page.

is the set of vertices and $E \subseteq V \times V$ is the set of edges. Given a set of M agents $\mathcal{A} = \{a_1, a_2, \dots, a_M\}$, each agent $a_i \in \mathcal{A}$ is assigned a start $s_i \in V$ and a goal $g_i \in V$. During planning, time is discretized into uniform time steps. At each time step, an agent executes an action, which is either to remain at its current vertex or move to an adjacent vertex. A solution to MAPF is a set of paths, one for each agent, satisfying the following *collision-avoidance constraints*: (1) *Vertex conflict avoidance*: No two agents occupy the same vertex at the same time step. (2) *Edge conflict avoidance*: No two agents traverse the same edge in opposite directions during the same time step. The MAPF under Real-world Deadlines (MAPF-RD) problem extends MAPF problem by considering agents' actual execution times and deadline constraints.

Definition 2 (MAPF with Real-world Deadlines): In the MAPF-RD problem, each agent a_i is given a deadline $T_i^D \in \mathbb{R}^+$. In addition to planning collision-free paths, each agent must execute its path under realistic conditions that account for robot dynamics, including kinodynamic constraints (e.g., velocity and acceleration limits), controller variability, and communication delays. Let $t_i \in \mathbb{R}^+$ denote the *execution time*, i.e., the wall clock time at which agent a_i reaches its goal during execution. To evaluate adherence to each agent's deadline constraint, we define a penalty function $\phi_i(t_i, T_i^D)$ that quantifies tardiness beyond the deadline T_i^D .

In this paper, we define two types of penalty functions: (1) *Linear penalty*: $\phi_i^L = \max(0, t_i - T_i^D)$, (2) *Percentage penalty*: $\phi_i^P = \mathbb{I}[t_i > T_i^D]$. Here, $\mathbb{I}[\cdot]$ denotes the indicator function, which returns 1 when agent a_i misses its deadline (i.e., $t_i > T_i^D$) and 0 otherwise. The *Linear penalty* captures the total tardiness, reflecting that longer delays typically incur higher costs in real-world applications. While *Percentage penalty* counts missed deadlines and focuses on the overall task completion rate. The objective of MAPF-RD is to compute a collision-free solution \mathcal{P} that minimizes the average penalty over all agents: $\frac{1}{M} \sum_{i=1}^M \phi_i(t_i, T_i^D)$.

B. Related Works

We first introduce existing methods for solving MAPF. Next, we discuss methods that address deadline constraints and those that bridge the gap between planning and real-world execution. Finally, we review learning-based techniques for predicting path execution time in MAPF and related domains.

1) *Multi-Agent Path Finding*: MAPF has received significant attention in recent years, resulting in a wide range of solvers. These methods can be broadly categorized based on their solution quality. Leading methods that produce high-quality solutions primarily belong to two families: the Conflict-Based Search (CBS) family [8]–[10] and the Large Neighborhood Search (LNS) family [11]–[13]. CBS incrementally builds solutions by generating plans that may initially contain collisions, then systematically resolving conflicts through constraint addition until a collision-free plan is obtained, with optimality or bounded suboptimality guarantees. LNS begins with a feasible, collision-free solution and iteratively improves solution quality by replanning for selected groups of agents in an unbounded suboptimal manner. Other

methods, including learning-based approaches [14], [15] and priority-based methods such as PIBT [16], offer improved scalability but typically produce solutions with lower quality. These methods form the foundation for many state-of-the-art MAPF solvers.

2) *MAPF with Deadlines*: MAPF with Deadlines (MAPF-DL) [5] is a variant of MAPF that focuses on time-constrained task completion. Several methods have been proposed to address this problem. Some formulate MAPF-DL as an optimization problem and solve it using network flow or integer linear programming [5], [17]. Others adapt existing search-based MAPF methods, such as CBS, MAPF-LNS, to handle deadline constraints [5], [18]. Recent extensions have further expanded the problem scope by incorporating task assignments [4], [19]. Despite varied models and strategies, all these methods define deadlines using the same discrete timesteps as the MAPF model. However, in practice, real-world deadlines are specified in wall-clock time, creating a mismatch between the abstract MAPF representation and actual execution requirements. This abstraction ignores critical factors such as velocity variations, turning costs, and execution uncertainty, which significantly impact actual completion times in robotic systems.

3) *Bridging Planning and Execution*: To bridge the gap between MAPF planning and real-world execution, several strategies have been explored. Some methods incorporate more accurate robot models during planning [7], [20]. However, these methods often struggle with scalability due to the complexity of the underlying models. Other methods use a decoupled pipeline where a discrete MAPF solution is first computed and then converted into executable trajectories through temporal scheduling or curve fitting [6], [21]. Building on this idea, some works have focused on robust execution of MAPF solutions [22]. The state-of-the-art execution framework is the Action Dependency Graph (ADG) [1].

An ADG is a directed graph that encodes dependencies among actions from a MAPF solution. Each vertex in the ADG contains a single action taken by an agent, and edges represent precedence constraints that must be respected during execution. The edge set consists of two types: *Type-1 edges* connect consecutive actions of the same agent, preserving the sequential order of its plan. *Type-2 edges* capture inter-agent dependencies at shared vertices, enforcing passing order constraints. Formally, a type-2 edge from action u to action v indicates that the agent assigned to v may begin its action only after the agent assigned to u has completed its execution. Given a MAPF plan, we construct an ADG by adding directed edges that encode both intra-agent sequential constraints and inter-agent passing orders at shared locations. During execution, agents proceed asynchronously while respecting these edge constraints. Although the ADG guarantees that all agents will eventually reach their goal vertices without collisions, it does not specify when this will occur. In fact, computing each agent's exact arrival time is non-trivial and typically requires running a simulation, which can be computationally expensive.

4) *Travel and Action Time Prediction*: Recent works have explored incorporating learning-based methods to predict action time during execution. One line of research focuses on predicting congestion-related delay in execution, includ-

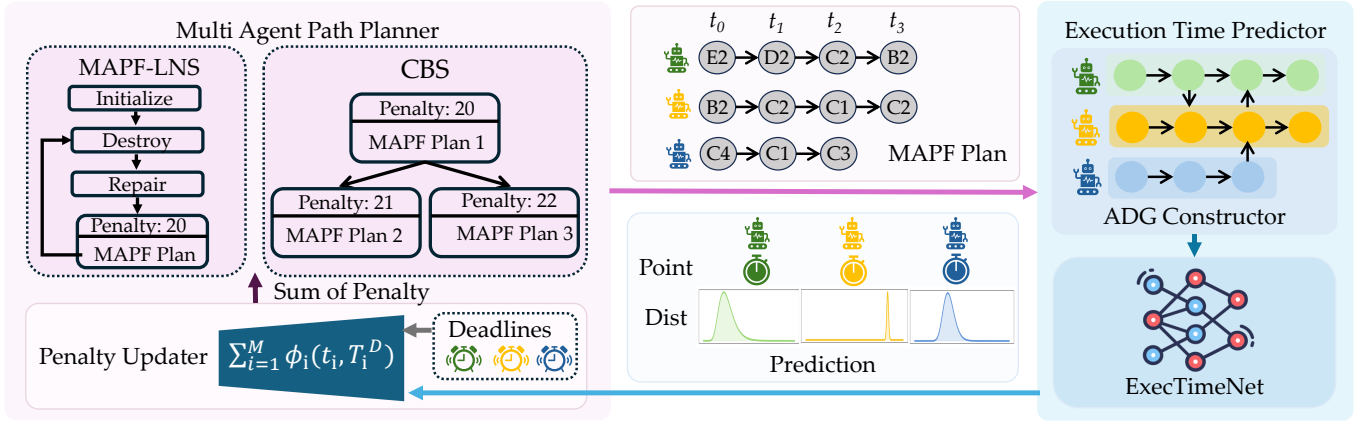


Fig. 1: Overview of REMAP.

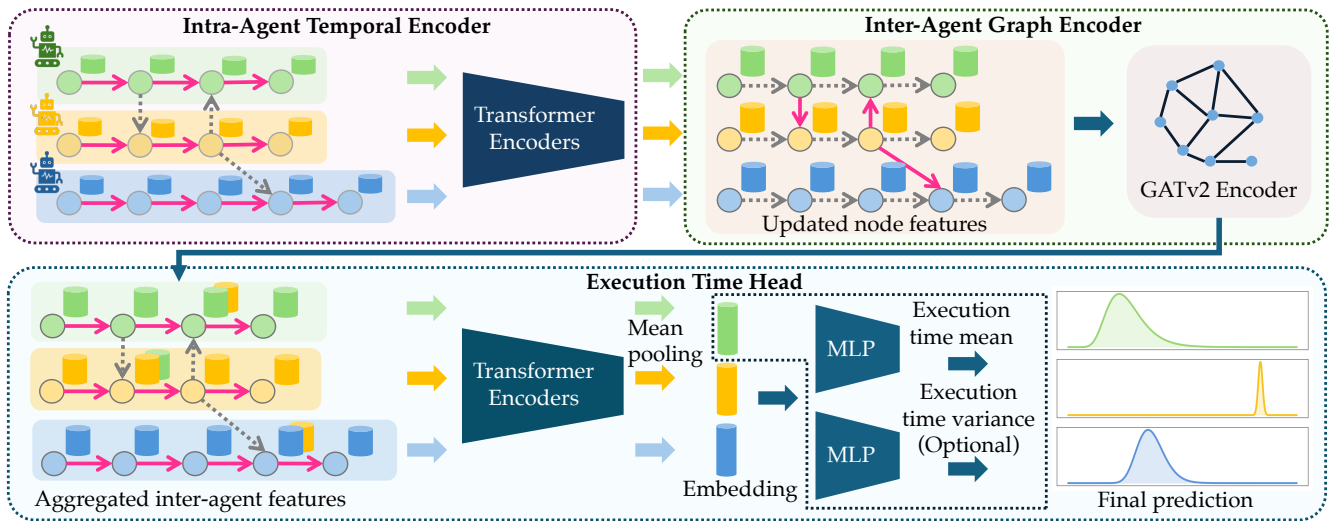


Fig. 2: Model structure of ExecTimeNet. Pink arrows indicate the direction of information propagation.

ing congestion prediction for large robot fleets [23] and congestion-aware models for planning under uncertainty [19]. Another direction uses learning-based methods to develop adaptive planners that update travel time estimates based on execution feedback [24]. Similar prediction techniques have been applied in related domains, such as highway traffic forecasting [25], train delay prediction [26], and Google Maps ETA prediction using graph neural networks [27]. However, these methods typically rely on local features or focus solely on the historical information of individual agents. In MAPF, delays can propagate across multiple agents and actions. By leveraging the structural information used during MAPF execution, we can build models that better account for these complex multi-agent dependencies.

III. METHOD

In this section, we first present an overview of our framework REMAP, which integrates execution-time prediction into the planning process. We then describe its key component, the execution-time predictor ExecTimeNet, in detail.

A. REMAP

REMAP facilitates dynamic interaction between MAPF planners and an execution-time predictor during the search process. The key insight is to use learned execution time predictions to guide the search toward solutions that are more likely to meet deadlines in practice. The overall structure is shown in Fig. 1. The core idea is straightforward: whenever the planner generates a set of paths, it builds an ADG based on the paths and then queries ExecTimeNet to estimate the execution time for each agent. This information is then used to guide the search of the planner. ExecTimeNet can provide two types of execution time information: (1) the time point for each agent to finish executing its path. (2) probability distributions over execution times, which capture the uncertainty inherent in real-world execution. This information is then returned to the planner, which uses it to compute penalties and guide the search toward solutions that optimize the objective of MAPF-RD. Note that our framework requires MAPF planners that can provide MAPF solutions during search, regardless of collisions. This capability is available in mainstream CBS and LNS algorithms and their variants, which cover most existing

MAPF methods. For joint search algorithms like M* [28], our approach can also be applied by assuming agents follow their shortest paths from the current configuration to the goals, though such planners are not the main focus of this work and we choose CBS and LNS families as representative examples to demonstrate our framework.

The remainder of this section is organized as follows: we first define the penalty computation procedures for both types of execution-time predictions. We then present the integration of REMAP with two representative MAPF planners from the CBS and LNS families: CBS and MAPF-LNS.

1) *Penalty Update*: Once execution times are predicted, the planner first uses them to compute deadline violation penalties. Concretely, if the estimation of execution time points $\{t_1, t_2, \dots, t_M\}$ are given, we calculate the sum of penalties exactly as described in Section II-A. If, instead, ExecTimeNet provides probability distributions $p_1(t), p_2(t), \dots, p_M(t)$ over execution times, we define the penalty for each agent as its expected penalty: (1) *Linear penalty*: $\phi_i(T_i, d_i) = \int_{d_i}^{\infty} (t - d_i) p_i(t) dt$, (2) *Percentage penalty*: $\phi_i(T_i, d_i) = \int_{d_i}^{\infty} p_i(t) dt = P(T_i > d_i)$.

2) *MAPF-LNS*: MAPF-LNS [11] employs large neighborhood search to solve MAPF problems in an unbounded suboptimal manner. The method first uses Prioritize Planning (PP) as initial solver to generate collision-free paths for all agents, then iteratively performs replanning over subsets of agents to improve solution quality. In each replanning iteration, the method selects a subset of agents called a neighborhood and replans their paths using prioritized planning. The newly generated paths must avoid collisions with each other and with the paths of all remaining agents. The method adopts the new paths only if they reduce the specified objective in MAPF-RD. Our framework integrates with MAPF-LNS by querying the ExecTimeNet after each replanning step, using the updated MAPF solution to obtain execution-time estimates for penalty computation. We also replace the original neighborhood selection strategies with a failure-aware neighborhood selection strategy that prefers selecting agents with frequent deadline violations to better reflect our objective. Details are provided in the appendix.

3) *CBS*: CBS [8] is a bi-level search-based method that finds optimal solutions for MAPF problems. The high-level search maintains an open list of nodes, where each node contains a set of constraints and a MAPF solution that follows these constraints but may still contain collisions. The low-level is a single-agent planner that computes shortest paths for each agent under given constraints. CBS begins by generating shortest paths for all agents without any constraints at the root node. When a collision is detected at a node, CBS resolves it by branching into child nodes, each adding a constraint that prevents one of the colliding agents from occupying the colliding location at the colliding time. Nodes in the open list are sorted according to the specified objective, and CBS terminates when a collision-free node is expanded. Our framework integrates CBS by querying ExecTimeNet with the MAPF solution in each node to replace path length with realistic execution time estimates. When constructing the ADG from CBS nodes that may contain collisions, collisions are

naturally encoded in the graph structure: vertex conflicts result in bidirectional Type-2 edges at the conflicting location, while edge conflicts create cyclic dependencies. This allows ExecTimeNet to estimate execution times that account for collision-induced delays without requiring explicit conflict resolution.

B. Execution Time Prediction (*ExecTimeNet*)

Given a set of paths, the objective of ExecTimeNet is to predict the *execution time* for each agent. We first build an ADG based on the MAPF plan. Next, we encode the ADG with edge and node features to create a representation compatible with the neural-network. This ADG-based encoding is independent of the underlying map layout, allowing the model to generalize across different maps. Finally, we use ExecTimeNet to predict the execution time for each agent.

1) *ADG encoding*: Given a set of paths, we first construct an ADG to capture the agent passing order, following the method in [29]. We then augment the ADG by attaching feature vectors to each node and edge, enabling its use as input to our neural network. This representation preserves the original topology of the ADG while enhancing its expressiveness. Concretely, we design three categories of features: (1) action features, (2) graph structural features, and (3) edge features. Each node is associated with an 11-dimensional feature vector that incorporates both action features and graph structural features. The action features include the action type (e.g., move forward or in-place rotation), the discrete time step from the MAPF plan, and the associated agent identifier. To capture the topological significance of each node, we define the following graph structural features: (1) the action's index in its agent's path, (2) the number of incoming and outgoing edges, reflecting causal dependencies; (3) the cumulative number of preceding actions and the cumulative number of future actions of the same type by the same agent; and (4) a binary indicator denoting whether the node has any outgoing type-2 edges, which indicates whether other agents' actions depend on this node. Each edge is associated with a 3-dimensional feature vector capturing: (1) the edge type (type-1 or type-2); (2) the relative index difference between connected nodes; and (3) the difference in scheduled execution times between the connected actions as given by the MAPF plan.

2) *ExecTimeNet Model*: Given the graph encoded from the ADG, predicting execution times presents two main challenges. First, it introduces complex temporal dependencies along type-1 edges: actions at earlier nodes can propagate delays that affect the execution times of latter nodes' actions. Second, it introduces complex inter-agent dependencies along type-2 edges: the execution of one agent's action directly constrains the timing of another's. These dependencies are often non-local and span multiple hops in the graph. Thus, traditional sequential or time-series prediction models are inadequate. To address these challenges, we propose ExecTimeNet, as shown in Fig. 2. The model is composed of three components: (1) an *Intra-Agent Temporal Encoder* that captures the long-range temporal dependencies within each agent's action sequence, (2) an *Inter-Agent Graph Encoder* that captures dependencies across agents using the graph

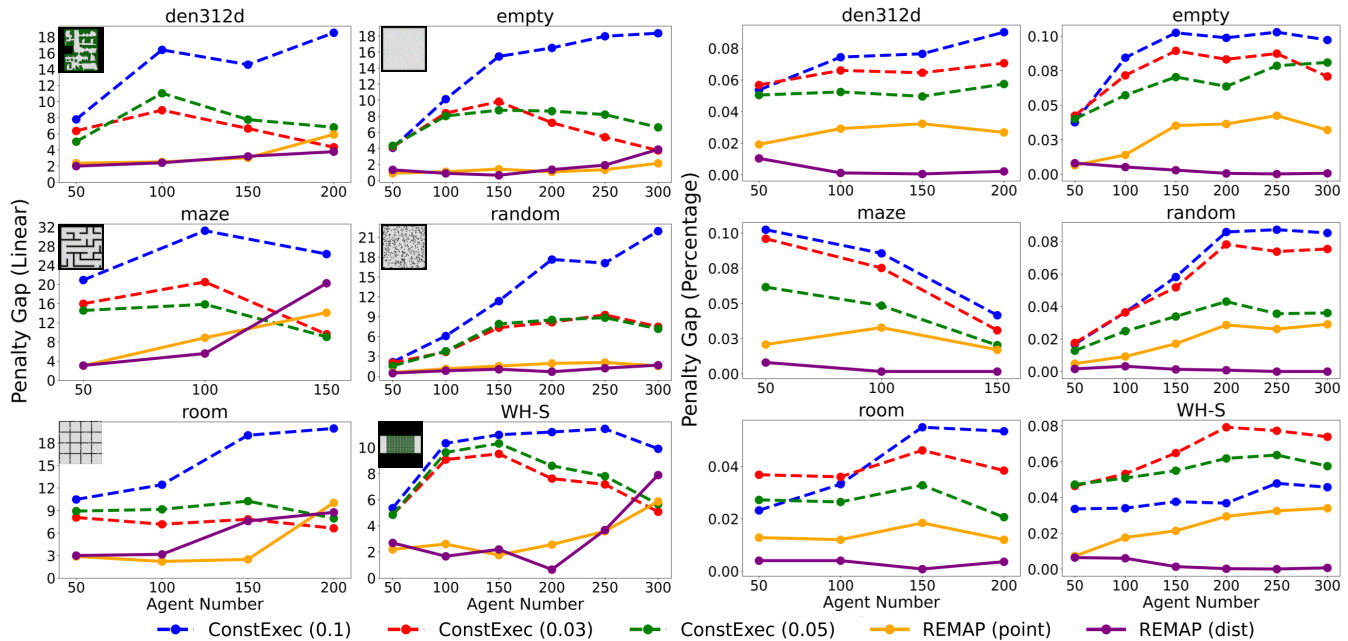


Fig. 3: Comparison of the linear and percentage penalty on MAPF-LNS. The terms “Linear” and “Percentage” in parentheses after “Penalty Gap” indicate the penalty types used in the planner.

structure, and (3) an *Execution Time Head* that generates either time point estimates or distributions of execution time predictions.

Given the encoded graph, we first use the *Intra-Agent Temporal Encoder* to capture temporal dependencies for the action sequence of each agent. Concretely, we treat the sequence of nodes corresponding to a single agent as an ordered trajectory and apply a Transformer [30] encoder to update the feature of each node by attending to all other actions from the same agent. This enables the model to capture long-range temporal dependencies, regardless of their distance in the graph. Next, we pass the graph with updated node features to the *Inter-Agent Graph Encoder*, which leverages a GATv2 [31] to propagate information across edges while incorporating edge features. This allows the model to account for inter-agent interactions, where the execution of one agent’s action can affect the timing of others through direct or indirect interactions. Finally, we use an *Execution Time Head* to generate predictions. Specifically, we use another Transformer encoder to aggregate the fused features across each agent’s nodes, followed by mean pooling to produce an embedding per agent. Based on it, ExecTimeNet predicts either: (1) the *exact execution time*, trained with the Mean Absolute Percentage Error (MAPE): $\mathcal{L}_{\text{MAPE}} = 1/|M| \cdot \sum_{i \in M} |(t_i - \hat{t}_i)/t_i|$, where t_i and \hat{t}_i denote the ground-truth and predicted execution times for agent a_i , respectively; or (2) the *execution time distribution*, modeled as a log-normal distribution. This choice reflects the fact that execution times are strictly positive and often show right-skewed variability due to factors such as delay propagation. To model this, the predictor outputs two values for each agent: the mean and standard deviation of a normal distribution in log space. The model is trained using the Gaussian negative log-likelihood loss [32].

TABLE I: MAPE (%) across (1) GNNExecNet, (2) LSTMExecNet, (3) ExecTimeNet (point), and (4) ExecTimeNet (dist). We mark out-of-distribution maps with (*)

Map	M	(1)	(2)	(3)	(4)
empty	50	4.0 ± 0.8	6.7 ± 1.1	3.2 ± 0.6	3.0 ± 0.6
	100	4.8 ± 0.5	7.4 ± 0.6	3.7 ± 0.5	3.5 ± 0.5
	150	4.9 ± 0.4	7.2 ± 0.6	3.9 ± 0.3	3.8 ± 0.3
	200	4.9 ± 0.3	6.8 ± 0.5	4.1 ± 0.3	3.9 ± 0.3
	300	4.9 ± 0.3	5.8 ± 0.5	4.0 ± 0.3	3.8 ± 0.3
WH-S	50	6.7 ± 0.8	9.9 ± 1.4	5.6 ± 0.9	4.9 ± 0.7
	100	6.8 ± 0.8	11.1 ± 1.2	5.4 ± 0.6	5.1 ± 0.6
	150	6.9 ± 0.4	11.7 ± 1.1	5.3 ± 0.5	5.5 ± 0.5
	200	7.2 ± 0.5	12.1 ± 1.3	5.4 ± 0.4	5.6 ± 0.5
	300	7.7 ± 0.6	13.0 ± 1.2	5.5 ± 0.4	5.8 ± 0.4
WH-L*	50	9.7 ± 1.3	12.6 ± 1.6	6.0 ± 0.8	8.0 ± 0.9
	100	10.2 ± 0.9	14.5 ± 1.6	6.7 ± 0.8	7.5 ± 0.8
	150	10.2 ± 0.8	14.8 ± 1.0	6.7 ± 0.5	6.9 ± 0.5
	200	10.0 ± 0.6	14.8 ± 1.2	6.9 ± 0.5	6.8 ± 0.5
	300	10.0 ± 0.5	14.5 ± 0.8	6.7 ± 0.4	6.3 ± 0.3
boston*	50	5.3 ± 0.7	8.4 ± 1.3	4.5 ± 0.4	3.9 ± 0.4
	100	5.9 ± 0.6	10.0 ± 0.7	4.0 ± 0.4	3.8 ± 0.4
	150	6.4 ± 0.6	11.2 ± 0.7	3.9 ± 0.4	3.9 ± 0.4
	200	6.7 ± 0.4	12.0 ± 0.6	3.9 ± 0.3	4.0 ± 0.3
	300	6.9 ± 0.4	13.2 ± 0.5	4.1 ± 0.3	4.2 ± 0.3
random	50	4.0 ± 0.6	6.5 ± 1.1	3.3 ± 0.6	3.5 ± 0.6
	100	4.5 ± 0.4	6.7 ± 0.8	3.7 ± 0.4	3.9 ± 0.4
	150	4.6 ± 0.4	6.4 ± 0.6	4.0 ± 0.4	3.9 ± 0.4
	200	4.7 ± 0.4	6.0 ± 0.5	4.0 ± 0.3	3.8 ± 0.3
	300	4.5 ± 0.3	5.0 ± 0.4	3.9 ± 0.3	3.7 ± 0.3

IV. EMPIRICAL EVALUATION

All experiments are conducted on an Ubuntu 20.04 system equipped with an AMD 3990X processor, 188 GB of RAM, and an NVIDIA 3090 Ti GPU. We use SMART [33] to

TABLE II: Feature importance analysis: impact of removing action, graph structure, and edge features.

Feature Configuration	MAPE (%)	Δ MAPE (%) \downarrow
Full Model (All Features)	4.18	-
w/o Action Features	4.34	0.16
w/o Graph Structural Features	5.34	1.16
w/o Edge Features	5.00	0.82

obtain the execution time in realistic simulation environment. SMART is an ADG-based, scalable realistic testbed for benchmarking MAPF algorithms under execution uncertainty and robot dynamics at a thousand-robot scale. In our experiments, each agent is subject to a speed limit of $[0, 5]$ m/s, an acceleration limit of $[-0.1, 0.1]$ m/s², and an angular velocity limit of $[0, 3]$ °/s. Each grid cell corresponds to 1×1 m. We use eight maps from the MovingAI Benchmark [34]: *empty* (empty-32-32, size: 32×32), *maze* (maze-32-32-4, size: 32×32), *random* (random-64-64-10, size: 64×64), *room* (room-64-64-16, size: 64×64), *den312d* (size: 65×81), *WH-S* (small) (warehouse-10-20-10-2-1, size: 161×63), *WH-L* (large) (warehouse-20-40-10-2-1, size: 321×123), and *boston* (Boston_0_256, size: 256×256). This section is organized as follows. We first evaluate the performance of ExecTimeNet, and then evaluate REMAP with two MAPF planners.

A. ExecTimeNet Evaluation

We first describe the training procedure for ExecTimeNet, then evaluate it on in- and out-of-distribution data, and finally conduct an ablation study to assess feature importance.

1) *Data Collection and Model Training*: To train ExecTimeNet, we first collect MAPF solutions from six maps: *empty*, *maze*, *random*, *room*, *den312d*, and *WH-S*. For each map, we use MAPF-LNS [11] to plan all 25 random instances with agent counts ranging from 10 to 300, saving the plan at every iteration to obtain multiple MAPF solutions per run. These plans are executed in SMART to obtain real-world execution times as training labels. Simultaneously, we extract encoded graphs from the ADGs constructed for each plan to use as input features. In total, we collect 9,433 graphs for training.

In our ExecTimeNet implementation, two transformer encoder blocks are employed, each consisting of 3 layers with 4 attention heads and a feedforward dimension of 256. We apply positional encoding to capture sequential information within each agent’s action sequence. The transformer layers use pre-layer normalization and a dropout rate of 0.1 for improved stability. Between the transformer blocks, two GATv2 graph convolutional layers with 64 hidden units process the graph structure with edge features. For the distribution prediction variant, we use two separate 4-layer MLPs to predict the mean and variance; only the mean MLP is used in the time-point prediction variant. Training is conducted using the Adam optimizer with a learning rate of 3×10^{-4} .

2) *Results on ExecTimeNet*: In this section, we evaluate the performance of ExecTimeNet by comparing it with two

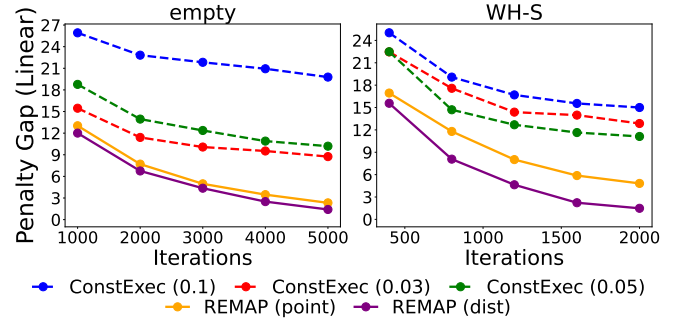


Fig. 4: Comparison of the linear penalty on MAPF-LNS with different iterations of refinement.

baseline methods: (1) GNNExecNet: inspired by [35], uses a graph neural network with two GATv2 layers to predict execution time based on the ADG, and (2) LSTMExecNet: following [23], processes each agent’s action sequence independently using LSTM models to predict execution times. We denote the time-point estimate variant as ExecTimeNet (point), and the probability distribution variant as ExecTimeNet (dist). Performance is measured using MAPE, which measures the prediction error as a percentage of the actual execution time. We evaluate prediction accuracy under two settings: (1) *In-distribution*: we use new paths from the training maps to test interpolation, and (2) *Out-of-distribution*: we use two new maps *WH-L* and *boston* to test generalization. We further vary the number of agents and map sizes to ensure a comprehensive assessment across diverse path length distributions.

As shown in Table I, ExecTimeNet consistently achieves significantly lower MAPE than all baselines. Moreover, its performance remains stable when transitioning from in-distribution to out-of-distribution scenarios or when varying the number of agents, demonstrating strong generalization. Between the two baselines, GNNExecNet consistently outperforms LSTMExecNet, highlighting the importance of modeling inter-agent dependencies for accurate execution time prediction in MAPF.

3) *Ablation Study*: To evaluate the contribution of different feature groups, we conduct an ablation study by training ExecTimeNet with each group removed in turn. As shown in Table II, removing graph structure features leads to the most significant increase in MAPE, indicating their critical role in capturing inter-agent dependencies. Removing edge features or action features also increases error, though to a lesser extent, indicating that these features provide complementary information. Overall, these results underscore the importance of modeling both spatial structure and edge-level interactions for accurate execution time prediction.

B. REMAP Evaluation

We evaluate our approach and baselines on six MovingAI Benchmark maps with 25 random instances. We refer to the two variants of REMAP as REMAP (point) for time-point predictions and REMAP (dist) for distributional predictions.

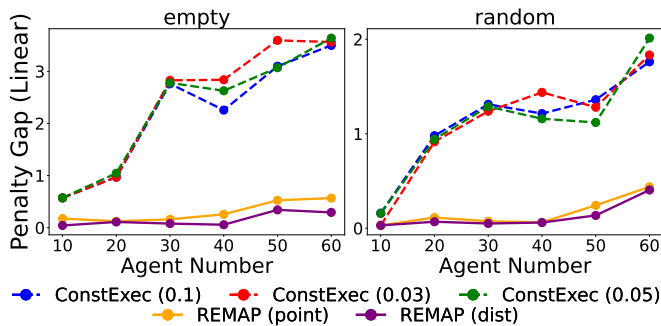


Fig. 5: Comparison of the linear penalty on CBS.

1) *Experiment Setting*: Inspired by [4], we design three baselines that estimate execution time using a constant execution-adjusted speed, defined as $u_e = K_u \cdot \bar{u}$, where \bar{u} is the maximum speed of agents and K_u is a scaling factor accounting for real-world execution effects. Execution time is then calculated as the path length divided by u_e . Based on simulation analysis, we use three values for K_u : 0.1, 0.05, and 0.03. The value 0.05 closely matches the mean observed ratio of path length to execution time, while 0.1 and 0.03 serve as upper and lower bounds. We refer to these baselines as ConstExec (0.1), ConstExec (0.05), and ConstExec (0.03), respectively. For each benchmark instance, we generate deadlines for each agent by first calculating the lower-bound execution time as the individual shortest path length divided by \bar{u} . This value is then multiplied by a scaling factor sampled from a uniform distribution $[K_D, K_D + 3]$, where K_D is a hyperparameter (see Appendix for selection details). We evaluate instances with agent counts ranging from 50 up to the largest number for which MAPF-LNS and CBS can achieve a 100% success rate within 60 seconds on each map. For each MAPF plan, we simulate their execution in SMART and compare actual execution times to deadlines to compute penalties. For fair comparison, results are normalized using a Virtual Best Solver (VBS), which represents the best solution among all methods for each scenario. We report each method’s penalty gap relative to the VBS, divided by the number of agents.

2) *Results on REMAP with MAPF-LNS*: The results in Fig. 3 show the penalty gap to VBS for all methods with MAPF-LNS. Since the curve represents the average results across all test instances, reaching $y = 0$ means the method achieves the best performance on every test instance. Our method approaches $y = 0$ on many maps, demonstrating its effectiveness. Under the linear penalty, our methods outperform most baselines but experience some performance degradation as agent count increases. Under the percentage penalty, our methods consistently achieve superior performance across all instances and maps. Between the two variants, REMAP (dist) generally outperforms REMAP (point) under percentage penalty, while both perform similarly under linear penalty. We attribute the observed degradation at higher agent counts to increased inference and ADG construction times for ExecTimeNet, which limit the number of MAPF-LNS refinement iterations within the runtime budget. To verify this, we com-

TABLE III: Runtime breakdown. Columns 3 to 6 correspond to number of nodes in ADG, time for ADG construction, time for inference for ExecTimeNet, and total time, respectively.

Map	M	Nodes #	ADG build (ms)	Inference (ms)	Total (ms)
empty	50	2241	0.4 ± 0.0	6.6 ± 0.1	7.1 ± 0.1
	100	5000	1.0 ± 0.0	12.5 ± 0.1	13.5 ± 0.1
	300	16279	6.1 ± 0.2	49.4 ± 0.5	55.5 ± 0.7
WH-L	50	18003	3.8 ± 0.1	32.6 ± 0.1	36.4 ± 0.3
	100	38270	9.9 ± 0.4	69.5 ± 0.9	79.4 ± 1.0
	300	116345	38.3 ± 0.3	277.5 ± 2.3	315.8 ± 2.3

pared our method and the baseline on two maps with 300 agents using the same number of MAPF-LNS iterations and linear penalty. As shown in Fig. 4, when iteration counts are fixed, our methods consistently outperform the baselines.

3) *Results on REMAP with CBS*: As shown in Fig. 5, REMAP consistently outperforms all baselines, achieving the lowest penalty gaps across most instances and agent counts, with results often approaching $y = 0$. Both variants of our method perform similarly in this evaluation. It is important to note that CBS does not guarantee optimality for MAPF-RD, due to inherent uncertainty in execution time prediction and the suboptimality of the low-level solver. A detailed analysis is provided in the appendix.

4) *Runtime Analysis*: We report the time required for REMAP to construct ADGs and perform inference in Table III. REMAP efficiently constructs ADG and performs inference with reasonable computational overhead. While these processing times increase with agent count, they remain sufficiently fast to support the planner effectively. Under ideal conditions, even on the WH-L map with 300 agents, our method can support approximately 200 iterations in MAPF-LNS within 1 minute. These results suggest promising opportunities for further optimization. As shown in Fig. 4, our approach consistently outperforms baselines when iteration counts are equal. However, as discussed in Section IV-B2, the computational overhead of inference and ADG construction limits the total number of refinement iterations achievable within the time budget. Therefore, reducing these computational costs represents a key pathway for enhancing the performance of REMAP.

V. CONCLUSION

In this paper, we proposed REMAP, a planning framework for solving the MAPF-RD problem, where the goal is to find collision-free paths for multiple agents that satisfy execution-time constraints. REMAP uses ExecTimeNet, a neural network that leverages both inter-agent and intra-agent information to accurately estimate execution times from planned paths. The framework is compatible with leading search-based MAPF planners with minor modifications. We demonstrate its integration with two widely used planners, MAPF-LNS and CBS. Experimental results in realistic simulations show that REMAP improves solution quality by up to 20%. Importantly, our approach requires training only a single model that generalizes across different numbers of agents and unseen maps. Beyond MAPF-RD, our model can be applied to various

time-sensitive multi-agent problems by providing accurate and timely execution time predictions. The ability to bridge the gap between abstract planning and real-world execution opens new opportunities for developing more reliable and practical multi-agent systems.

REFERENCES

- [1] W. Hönl, S. Kiesel, A. Tinka, J. W. Durham, and N. Ayanian, "Persistent and robust execution of MAPF schedules in warehouses," *IEEE Robotics and Automation Letters*, vol. 4, no. 2, pp. 1125–1131, 2019.
- [2] J. Li, T. A. Hoang, E. Lin, H. L. Vu, and S. Koenig, "Intersection coordination with priority-based search for autonomous vehicles," in *Proceedings of the AAAI Conference on Artificial Intelligence*, vol. 37, 2023, pp. 11 578–11 585.
- [3] R. Morris, C. S. Pasareanu, K. Luckow, W. Malik, H. Ma, T. S. Kumar, and S. Koenig, "Planning, scheduling and monitoring for airport surface operations," in *AAAI Workshop: Planning for Hybrid Systems*, 2016.
- [4] T. Huang, V. Shivashankar, M. Caldara, J. W. Durham, J. Li, B. Dilkina, and S. Koenig, "Deadline-aware multi-agent tour planning," in *Proceedings of the International Conference on Automated Planning and Scheduling*, 2023, pp. 189–197.
- [5] H. Ma, G. Wagner, A. Felner, J. Li, T. K. S. Kumar, and S. Koenig, "Multi-agent path finding with deadlines," in *Proceedings of the International Joint Conference on Artificial Intelligence*, 2018, pp. 417–423.
- [6] W. Hönl, T. K. S. Kumar, L. Cohen, H. Ma, H. Xu, N. Ayanian, and S. Koenig, "Multi-agent path finding with kinematic constraints," in *Proceedings of the International Conference on Automated Planning and Scheduling*, vol. 26, 2016, pp. 477–485.
- [7] J. Yan and J. Li, "Multi-agent motion planning for differential drive robots through stationary state search," in *Proceedings of the AAAI Conference on Artificial Intelligence*, vol. 39, no. 22, 2025, pp. 23 360–23 368.
- [8] G. Sharon, R. Stern, A. Felner, and N. R. Sturtevant, "Conflict-based search for optimal multi-agent pathfinding," *Artificial Intelligence*, vol. 219, pp. 40–66, 2015.
- [9] J. Li, W. Ruml, and S. Koenig, "EECBS: A bounded-suboptimal search for multi-agent path finding," in *Proceedings of the AAAI Conference on Artificial Intelligence*, vol. 35, 2021, pp. 12 353–12 362.
- [10] J. Li, A. Felner, E. Boyarski, H. Ma, and S. Koenig, "Improved heuristics for conflict-based search for multi-agent path finding," in *Proceedings of the International Joint Conference on Artificial Intelligence*, 2019, pp. 442–449.
- [11] J. Li, Z. Chen, D. Harabor, P. J. Stuckey, and S. Koenig, "Anytime multi-agent path finding via large neighborhood search," in *Proceedings of the International Joint Conference on Artificial Intelligence*, 2021, pp. 4127–4135.
- [12] T. Huang, J. Li, S. Koenig, and B. Dilkina, "Anytime multi-agent path finding via machine learning-guided large neighborhood search," in *Proceedings of the AAAI Conference on Artificial Intelligence*, 2022, pp. 9368–9376.
- [13] J. Li, Z. Chen, D. Harabor, P. J. Stuckey, and S. Koenig, "MAPF-LNS2: Fast repairing for multi-agent path finding via large neighborhood search," in *Proceedings of the AAAI Conference on Artificial Intelligence*, vol. 36, 2022, pp. 10 256–10 265.
- [14] G. Sartoretti, J. Kerr, Y. Shi, G. Wagner, T. K. S. Kumar, S. Koenig, and H. Choset, "Primal: Pathfinding via reinforcement and imitation multi-agent learning," *IEEE Robotics and Automation Letters*, vol. 4, no. 3, pp. 2378–2385, 2019.
- [15] M. Damani, Z. Luo, E. Wenzel, and G. Sartoretti, "Primal₂: Pathfinding via reinforcement and imitation multi-agent learning - lifelong," *IEEE Robotics and Automation Letters*, vol. 6, no. 2, pp. 2666–2673, 2021.
- [16] K. Okumura, M. Machida, X. Défago, and Y. Tamura, "Priority inheritance with backtracking for iterative multi-agent path finding," *Artificial Intelligence*, vol. 310, p. 103752, 2022.
- [17] H. Wang and W. Chen, "Multi-robot path planning with due times," *IEEE Robotics and Automation Letters*, vol. 7, no. 2, pp. 4829–4836, 2022.
- [18] J. Li, Z. Chen, Y. Zheng, S.-H. Chan, D. Harabor, P. J. Stuckey, H. Ma, and S. Koenig, "Scalable rail planning and replanning: Winning the 2020 flatland challenge," in *Proceedings of the International Conference on Automated Planning and Scheduling*, 2021, pp. 477–485.
- [19] G. Fine, D. Atzmon, and N. Agmon, "Anonymous multi-agent path finding with individual deadlines," in *Proceedings of the International Conference on Autonomous Agents and Multi-agent Systems*, 2023, pp. 869–877.
- [20] J. Kottlinger, S. Almagor, and M. Lahijanian, "Conflict-based search for multi-robot motion planning with kinodynamic constraints," in *Proceedings of the IEEE International Conference on Intelligent Robots and Systems*, 2022, pp. 13 494–13 499.
- [21] H. Zhang, N. Tiruvilumala, S. Koenig, and T. S. Kumar, "Temporal reasoning with kinodynamic networks," in *Proceedings of the International Conference on Automated Planning and Scheduling*, vol. 31, 2021, pp. 415–425.
- [22] M. Čáp, J. Gregoire, and E. Frazzoli, "Provably safe and deadlock-free execution of multi-robot plans under delaying disturbances," in *Proceedings of the IEEE International Conference on Intelligent Robots and Systems*, 2016, pp. 5113–5118.
- [23] G. Yu and M. T. Wolf, "Congestion prediction for large fleets of mobile robots," in *Proceedings of the IEEE International Conference on Robotics and Automation*, 2023, pp. 7642–7649.
- [24] A. Kita, N. Suenari, M. Okada, and T. Taniguchi, "Online re-planning and adaptive parameter update for multi-agent path finding with stochastic travel times," *arXiv preprint*, vol. arXiv:2302.01489, 2023.
- [25] C. Song, Y. Lin, S. Guo, and H. Wan, "Spatial-temporal synchronous graph convolutional networks: A new framework for spatial-temporal network data forecasting," in *Proceedings of the AAAI Conference on Artificial Intelligence*, vol. 34, no. 01, 2020, pp. 914–921.
- [26] H. Wen, Y. Lin, F. Wu, H. Wan, Z. Sun, T. Cai, H. Liu, S. Guo, J. Zheng, C. Song *et al.*, "Enough waiting for the couriers: Learning to estimate package pick-up arrival time from couriers' spatial-temporal behaviors," *ACM Transactions on Intelligent Systems and Technology*, vol. 14, no. 3, pp. 1–22, 2023.
- [27] A. Derrow-Pinion, J. She, D. Wong, O. Lange, T. Hester, L. Perez, M. Nunkesser, S. Lee, X. Guo, B. Wiltshire *et al.*, "ETA prediction with graph neural networks in Google Maps," in *Proceedings of the 30th ACM International Conference on Information & Knowledge Management*, 2021, pp. 3767–3776.
- [28] G. Wagner and H. Choset, "Subdimensional expansion for multirobot path planning," *Artificial Intelligence*, vol. 219, pp. 1–24, 2015.
- [29] J. Dunkel, "Streamlining the action dependency graph framework: Two key enhancements," *arXiv preprint*, vol. arXiv:2412.01277, 2024.
- [30] A. Vaswani, N. Shazeer, N. Parmar, J. Uszkoreit, L. Jones, A. N. Gomez, E. Kaiser, and I. Polosukhin, "Attention is all you need," in *Advances in Neural Information Processing Systems*, 2017, pp. 5998–6008.
- [31] S. Brody, U. Alon, and E. Yahav, "How attentive are graph attention networks?" in *International Conference on Learning Representations*, 2022.
- [32] A. Kendall and Y. Gal, "What uncertainties do we need in Bayesian deep learning for computer vision?" in *Advances in Neural Information Processing Systems*, vol. 30, 2017, pp. 5574–5584.
- [33] J. Yan, Z. Li, W. Kang, Y. Zhang, S. Smith, and J. Li, "Advancing mapf towards the real world: A scalable multi-agent realistic testbed (smart)," *arXiv preprint*, vol. arXiv:2503.04798, 2025.
- [34] R. Stern, N. R. Sturtevant, A. Felner, S. Koenig, H. Ma, T. T. Walker, J. Li, D. Atzmon, L. Cohen, T. K. S. Kumar, E. Boyarski, and R. Barták, "Multi-agent pathfinding: Definitions, variants, and benchmarks," in *Proceedings of the International Symposium on Combinatorial Search*, 2019, pp. 151–159.
- [35] Y. Meng, N. Majcherczyk, W. Liu, S. Kiesel, C. Fan, and F. Pecora, "Reliable and efficient multi-agent coordination via graph neural network variational autoencoders," *arXiv preprint*, vol. arXiv:2503.02954, 2025.
- [36] S. Ropke and D. Pisinger, "An adaptive large neighborhood search heuristic for the pickup and delivery problem with time windows," *Transportation Science*, vol. 40, no. 4, pp. 455–472, 2006.

VI. APPENDIX

A. Data Collection for ExecTimeNet

As described in the main text, we collect MAPF plans from six maps: empty, maze, random, room, den312d, and WH-S. For each map, we use MAPF-LNS [11] to plan for all 25 random instances with a time limit of 60 seconds per run. We begin with 10 agents and increment the agent count by 10 for each run, continuing until reaching 300 agents or until more than 5 failed instances occur for a given agent count. During each run, we save the plan generated at every iteration, which can yield multiple MAPF plans per instance. Afterward, we process these plans and retain only those with unique solution costs (SoC). In total, we collect 9,433 MAPF plans.

These plans are then executed in SMART to obtain real-world execution times as training labels. At the same time, we extract encoded graphs from the ADGs constructed for each plan to serve as input features, resulting in 9,433 graphs for training. The entire simulation process takes approximately three days to complete.

B. Model Implementation Details

We present our detailed model structure in Fig. 6. Initially, node features are grouped by their associated agent id and projected to 64-dimensional hidden representations. We apply positional encoding to capture sequential information within each agent’s action sequence. Then, we pass each of these groups to a transformer encoder block consisting of 3 layers with 4 attention heads and a feedforward dimension of 256. The transformer layers use pre-layer normalization and a dropout rate of 0.1 for improved stability. Next, we flatten all groups back to a graph and integrate two GATv2 graph convolutional layers with 64 hidden units to process the graph structure with 3-dimensional edge features. Afterward, we regroup the node features and pass them through a transformer encoder with the same dimensions as before. Following the encoder, we apply masked mean pooling to aggregate sequence-level information across variable-length agent trajectories. For distribution prediction, the pooled representation is fed to two separate 4-layer MLPs that predict the mean μ and variance σ^2 of execution time, respectively. This dual-head design enables uncertainty quantification by modeling the runtime as a Gaussian distribution $\mathcal{N}(\mu, \sigma^2)$. In contrast, our time-point prediction variant employs only the mean prediction head for deterministic runtime estimation.

During training, we preprocess the label y to $\log(y)$, since execution times range from 10 to 3,000, s. During inference, we recover the predicted execution time by applying the exponential function. The entire pipeline is implemented using PyTorch Geometric and trained with the Adam optimizer at a learning rate of 3×10^{-4} . The total number of parameters for ExecTimeNet (dist) is 325,602.

C. MAPF-LNS w/ Quadratic Penalty

In addition to the two penalty settings proposed in the main text, we also evaluated an additional *Quadratic penalty*,

GNN Transformer Distribution Predictor

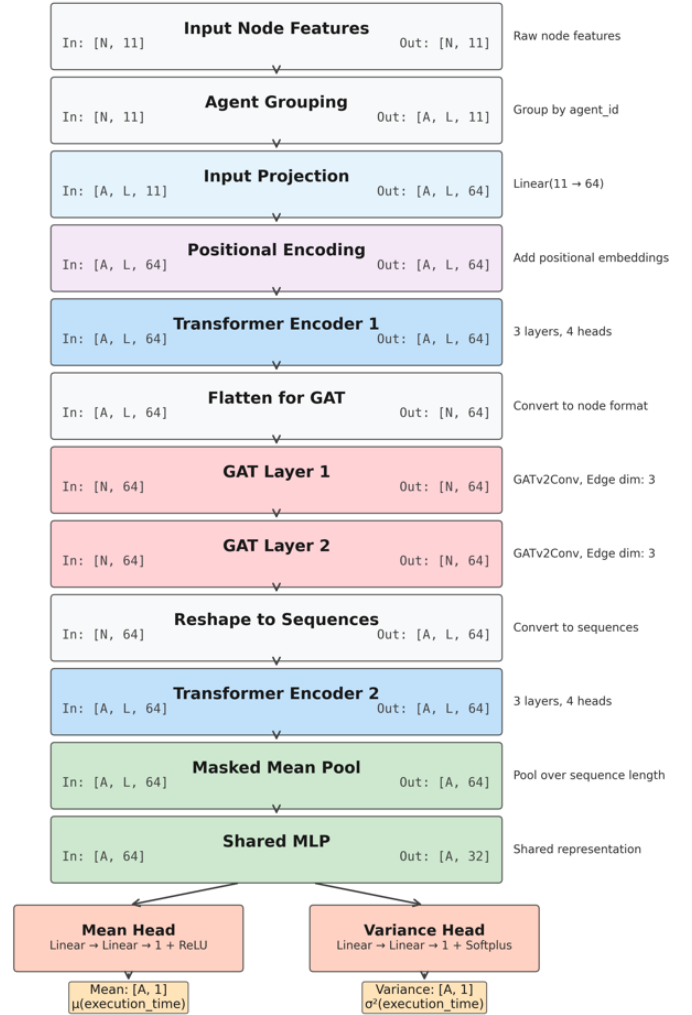


Fig. 6: Detailed model structure of ExecTimeNet (dist).

defined as follows: $\phi_i^Q = (\max(0, t_i - T_i^D))^2$. As shown in Fig. 7, REMAP outperforms baseline methods on most maps under this setting. However, since the overall trends and conclusions closely mirror those observed with the linear penalty, we present only the linear penalty results in the main text for brevity.

D. MAPF-LNS w/ Failure-based Neighbor Selection

In this section, we first review the MAPF-LNS neighborhood selection, and then introduce our proposed failure-based neighborhood. At last, we evaluate our proposed neighborhood’s performance through empirical experiment.

1) *Adaptive Neighborhood*: The original MAPF-LNS employs a set of three neighborhood and selects one of them in each iteration, namely an agent-based neighborhood, a map-based neighborhood and a random neighborhood. The agent-based neighborhood generation includes a seed agent a_j with the current maximum delay (the gap between current path length and individual shortest path length) and other agents,

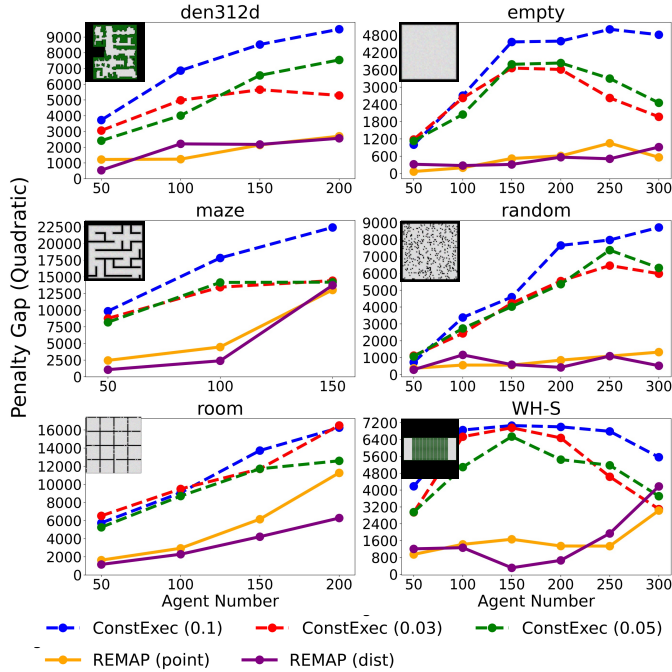


Fig. 7: Results on MAPF-LNS with quadratic penalty.

determined via a procedure random walks, that prevent a_j from achieving a lower delay. The map-based neighborhood randomly chooses a vertex $v \in V$ with a degree greater than 2 and generates a neighborhood of agents moving around v . The random heuristic performs a random uniform selection of N agents from the agent set. MAPF-LNS [11] employs an adaptive selection mechanism π that maintains selection weights to choose among different neighborhoods in each iteration [36]. Initially, all neighborhoods have equal selection probability. During the refinement process, when the new solution generated using a selected neighborhood achieves better cost than the previous solution, the corresponding neighborhood’s selection weight is increased, thereby enhancing its probability of being selected in future iterations.

MAPF-LNS neighborhoods were designed for MAPF. To address MAPF-RD, we designed a new neighborhood selection that is inspired by the agent-based neighborhood.

2) *Failure-based Neighborhood*: Failure-based neighborhood targets agents that frequently violate deadlines. We define a set of deadline violation counts $VC = \{vc_1, vc_2, \dots, vc_M\}$, initially set to zero for all agents. In each iteration, after obtaining predicted execution time points from ExecTimeNet and comparing them with deadlines, we update the violation counts as follows: for any agent $a_i \in M$, its deadline violation count vc_i increases by 1 if it violates the deadline, otherwise it is reset to 0. This real-time tracking enables the planner to identify agents that persistently fail to meet their deadline. During neighborhood selection, we perform softmax sampling that favors agents with higher deadline violation counts to select a seed agent a_j . A random walk [11] is then performed from a random position in the current path p_j to collect other agents a_i whose paths p_i intersect with the random walk, indicating their contribution to the deadline violation of a_j ,

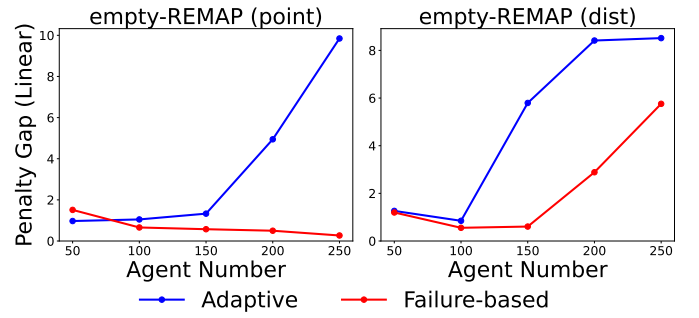


Fig. 8: Results on MAPF-LNS with different neighborhood selection.

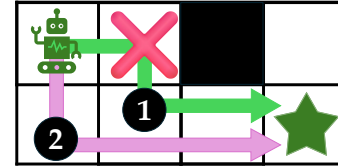


Fig. 9: Toy example to show that CBS under MAPF-RD is non-optimal.

thereby generating the neighborhood.

We evaluate our proposed failure-based neighborhood by comparing it against the adaptive neighborhood approach on the empty map. We conduct experiments using REMAP (point) and REMAP (dist) with both the adaptive neighborhood and failure-based neighborhood. As illustrated in Fig. 8, our failure-based neighborhood demonstrates superior performance compared to the adaptive neighborhood in the majority of test instances. Moreover, our method consistently achieves the smallest performance gap relative to the VBS, providing strong evidence of its effectiveness in addressing MAPF-RD.

E. Optimality of CBS in MAPF-RD Problem

CBS does not guarantee optimal solutions under the MAPF-RD setting. The reason is that our approach only considers the predicted execution time after the planner generates a MAPF plan, while the low-level single-agent path planning does not incorporate execution time considerations. Specifically, CBS’s low-level planner optimizes for the shortest path length rather than execution time, which can lead to suboptimal solutions in terms of deadline violations. In standard MAPF, CBS maintains optimality by ensuring that conflict resolution monotonically increases the objective function [8], namely the sum of path costs. However, this property no longer holds when execution time predictions are involved in the penalty calculation but are not directly optimized by the low-level planner. A concrete example illustrating this issue is provided in Fig. 9. Consider two paths of equal length, path 1 and path 2. When CBS resolves a conflict at the red X location in path 1, the low-level planner selects path 2 for the robot, which has the same length as path 1. However, path 2 requires fewer turns, leading to fewer acceleration and deceleration phases than path 1. This decreases execution time and may help meet

the deadline. Consequently, conflict resolution can decrease rather than increase the sum of penalties, violating CBS's monotonicity property. Moreover, the inaccuracy of execution time predictions further contributes to CBS's sub-optimality in our framework, as the the judgment of whether the agent has met deadline may be wrong. This limitation presents an interesting direction for future work: exploring how execution time considerations can be integrated directly into the low-level path planning process to restore optimality guarantees while maintaining computational efficiency.

F. Deadline Scaling Factor K_D

The deadline scaling factor K_D is important in deadline setting. If K_D is too small, the resulting deadlines become too tight, causing most agents to fail to meet their deadlines. Conversely, if K_D is too large, the deadlines become too loose, allowing most agents to easily meet their deadlines and leaving little room for the planning algorithm to demonstrate improvement. To select an appropriate value for K_D , we perform a grid search, varying K_D from 8 to 16 in steps of 2 to generate corresponding deadlines. For each setting, we run ConstExec (0.1) and record its percentage penalty across all maps and agent counts. We then choose the value of K_D that results in approximately 50% of agents meeting their deadlines for each map and agent counts. This ensures a balanced and meaningful evaluation across different scenarios.